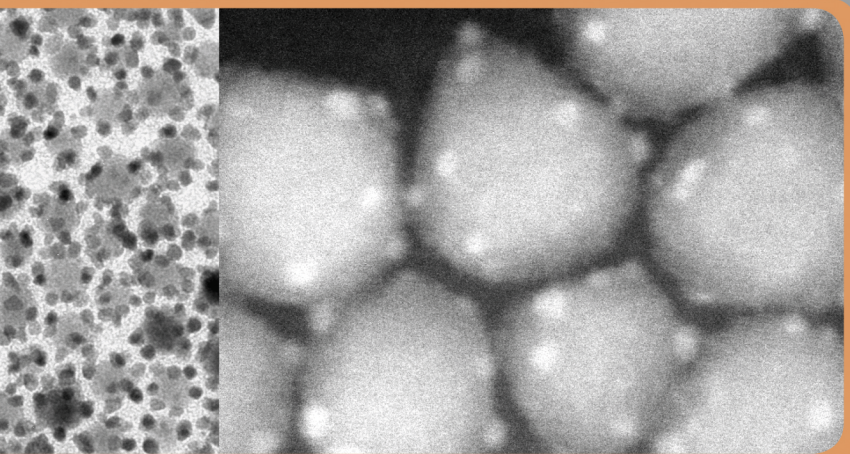


Michaela Meyns

Metal-semiconductor hybrid nanoparticles

Halogen induced shape control,
hybrid synthesis and electrical
transport



**Anchor Academic
Publishing**
disseminate knowledge

Meyns, Michaela: Metal-semiconductor hybrid nanoparticles. Halogen induced shape control, hybrid synthesis and electrical transport, Hamburg, Anchor Academic Publishing 2015

Buch-ISBN: 978-3-95489-293-8

PDF-eBook-ISBN: 978-3-95489-793-3

Druck/Herstellung: Anchor Academic Publishing, Hamburg, 2015

Bibliografische Information der Deutschen Nationalbibliothek:

Die Deutsche Nationalbibliothek verzeichnet diese Publikation in der Deutschen Nationalbibliografie; detaillierte bibliografische Daten sind im Internet über <http://dnb.d-nb.de> abrufbar.

Bibliographical Information of the German National Library:

The German National Library lists this publication in the German National Bibliography. Detailed bibliographic data can be found at: <http://dnb.d-nb.de>

All rights reserved. This publication may not be reproduced, stored in a retrieval system or transmitted, in any form or by any means, electronic, mechanical, photocopying, recording or otherwise, without the prior permission of the publishers.

Das Werk einschließlich aller seiner Teile ist urheberrechtlich geschützt. Jede Verwertung außerhalb der Grenzen des Urheberrechtsgesetzes ist ohne Zustimmung des Verlages unzulässig und strafbar. Dies gilt insbesondere für Vervielfältigungen, Übersetzungen, Mikroverfilmungen und die Einspeicherung und Bearbeitung in elektronischen Systemen.

Die Wiedergabe von Gebrauchsnamen, Handelsnamen, Warenbezeichnungen usw. in diesem Werk berechtigt auch ohne besondere Kennzeichnung nicht zu der Annahme, dass solche Namen im Sinne der Warenzeichen- und Markenschutz-Gesetzgebung als frei zu betrachten wären und daher von jedermann benutzt werden dürften.

Die Informationen in diesem Werk wurden mit Sorgfalt erarbeitet. Dennoch können Fehler nicht vollständig ausgeschlossen werden und die Diplomica Verlag GmbH, die Autoren oder Übersetzer übernehmen keine juristische Verantwortung oder irgendeine Haftung für evtl. verbliebene fehlerhafte Angaben und deren Folgen.

Alle Rechte vorbehalten

© Anchor Academic Publishing, Imprint der Diplomica Verlag GmbH
Hermannstal 119k, 22119 Hamburg
<http://www.diplomica-verlag.de>, Hamburg 2015
Printed in Germany

Contents

List of Abbreviations	ix
List of Figures	xi
List of Schemes	xiii
List of Tables	xiii
1 Introduction	1
2 Halogen induced shape control of CdSe nanoparticles	5
2.1 Properties and synthesis of semiconductor nanoparticles	6
2.1.1 Properties of semiconductor (CdSe) nanoparticles	6
2.1.2 Colloidal semiconductor nanoparticle synthesis and shape control	8
2.1.2.1 Basics of nanoparticle nucleation	9
2.1.2.2 Mechanisms of shape control	9
2.1.2.3 The hot injection synthesis and shape control	13
2.2 CdSe nanoparticle shape evolution tuned by halogenated additives	15
2.2.1 Effects of 1,2-dichloroethane on the synthesis of CdSe nanorods	15
2.2.2 Shape and size manipulation with other halogen compounds	20
2.2.2.1 Variation of the halogen additives	21
2.2.2.2 Size control by additive injection after the nucleation	24
2.2.3 Morphology related changes of phosphorous and halogen contents examined by surface and elemental analysis	24
2.2.4 Ligand-surface interactions and the hexagonal pyramidal shape	29
2.2.5 A closer look at the shape evolution process	34
2.3 Conclusions	37
3 Metal-semiconductor hybrid nanoparticles	39

3.1	Properties and synthesis of metal-semiconductor hybrid nanoparticles . . .	40
3.1.1	Properties of metal-semiconductor hybrid nanoparticles	40
3.1.2	Synthesis of metal-semiconductor hybrid nanostructures	43
3.1.2.1	Deposition of metallic domains	44
3.1.2.2	Ion exchange	48
3.2	Metal-CdSe nanopyramid hybrid structures - deposition and ion exchange .	50
3.2.1	Au-CdSe nanopyramid structures	52
3.2.1.1	Influence of the precursor oxidation state on the hybrid morphology	56
3.2.1.2	Compositional analysis by EDX and XPS	62
3.2.1.3	Reasons for the different deposition behaviour	68
3.2.1.4	Annealing of Au-CdSe shell monolayers	69
3.2.2	Reactions of CdSe nanopyramids with Ag, Pd and Pt	71
3.2.2.1	Reaction with Ag(I)	71
3.2.2.2	Reactions with Pd(II)	73
3.2.2.3	Reactions with Pt(II)	78
3.3	Conclusions	85
4	Electrical transport in hybrid nanoparticle films	87
4.1	Electrical transport in nanoparticle arrays	88
4.1.1	Transport mechanisms and photoconductivity	90
4.1.1.1	Coulomb blockade and single-electron transistor	90
4.1.1.2	Transport mechanisms in non-crystalline materials	91
4.1.1.3	Photoconductivity	93
4.1.2	Electrical transport in metal-semiconductor hybrid nanoparticles . .	93
4.1.2.1	Macroscopic metal-semiconductor contacts	94
4.1.2.2	Metal-semiconductor nanocontacts	95
4.2	Electrical transport in CdSe and Pt-CdSe nanoparticle devices	97
4.2.1	Electrical transport through pyramidal CdSe nanoparticles	98
4.2.2	Electrical transport through Pt-CdSe hybrid nanoparticles	101
4.2.2.1	Electrical transport in Pt-CdSe hybrid nanoparticles with 1.7 nm Pt domains	102
4.2.2.2	Electrical transport in Pt-CdSe hybrid nanoparticles with 3.2 nm Pt domains	103
4.3	Conclusions and perspective	111

5	Experimental	113
5.1	Materials and preparation methods	113
5.1.1	Materials	113
5.1.2	Synthesis of pyramidal CdSe nanocrystals	114
5.1.2.1	Standard recipe	114
5.1.2.2	Variation of the halogenated additives	114
5.1.2.3	Injection of 1-chlorooctadecane after CdSe nucleation . . .	115
5.1.2.4	Determination of the relative concentration of protons in aliquots	115
5.1.2.5	Samples for XPS	115
5.1.3	Synthesis of Au-CdSe pyramid hybrid nanoparticles	116
5.1.3.1	Gold(III)-stock solutions	116
5.1.3.2	CdSe dispersions	116
5.1.3.3	Au-CdSe hybrid nanoparticles with DCE-nanopyramids .	117
5.1.3.4	Au-CdSe hybrid nanoparticles with COD-nanopyramids .	118
5.1.4	Reactions of CdSe nanopyramids with Ag, Pd and Pt precursors . .	120
5.1.4.1	Silver	121
5.1.4.2	Palladium	121
5.1.4.3	Platinum	123
5.1.5	Langmuir-Blodgett monolayer preparation and annealing	124
5.1.5.1	Nanoparticle purification	124
5.1.5.2	Film preparation and annealing	125
5.2	Characterisation	126
5.2.1	Transmission Electron Microscopy (TEM), Energy Dispersive X-ray Spectroscopy (EDX)	126
5.2.2	UV-Visible absorption and fluorescence spectrometry	126
5.2.3	X-ray powder diffraction (XRD)	128
5.2.4	Scanning electron microscopy (SEM)	128
5.2.5	Total Reflection X-ray Fluorescence Spectroscopy (TXRF)	128
5.2.6	Attenuated Total Reflectance Fourier Transformation Infrared Spec- troscopy (ATR-FTIR)	129
5.2.7	X-ray Photoelectron Spectroscopy (XPS)	129
5.2.8	Electrical transport	130
6	Summary	131

7 Zusammenfassung	133
A Additional data	I
B Safety	VII
Bibliography	XXIII
Acknowledgements	LVII
Curriculum Vitae	LIX
Publications and conference contributions	LXI
Erklärungen	LXIII

List of Abbreviations

BE	Binding energy
CB	Conduction band
COD	1-Chlorooctadecane
Cub.	Cubic
DBE	Dibromoethane
DCE	1,2-Dichloroethane
DDA	Dodecylamine
DDT	Dodecanethiol
DEG	Diethyleneglycol
DFT	Density functional theory
DIE	1,2-Diiodoethane
DTAB	<i>n</i> -Dodecyltrimethylammonium bromide
DTAC	<i>n</i> -Dodecyltrimethylammonium chloride
EDX	Energy dispersive X-ray spectroscopy
FWHM	Full width at half maximum
Hex.	Hexagonal
HDA	Hexadecylamine
HOPG	Highly oriented pyrolytic graphite
ICP-OES	Inductively Coupled Plasma Optical Emission Spectroscopy
MIGS	Metal induced gap state
Monocl.	Monoclinic
NNH	Nearest-neighbour hopping
OAc	Oleic acid
OAm	Oleylamine
Orthorhomb.	Orthorhombic
PMMA	Polymethylmetacrylate
QY	Quantum yield

STEM	Scanning transmission electron microscopy
TBAB	Tetra- <i>n</i> -butylammonium borohydride
TCE	1,1,2-Trichloroethane
TEM	Transmission electron microscopy
Tetr.	Tetragonal
TOP(O)	Tri- <i>n</i> -octylphosphine (oxide)
TXRF	Total reflection X-ray fluorescence spectroscopy
UV-Vis	Ultraviolet-visible
VB	Valence band
VRH	Variable-range hopping
XPS	X-ray Photoelectron Spectroscopy
XRD	Powder X-ray diffractometry

List of Figures

2.1	Wurtzite crystal structure of CdSe	8
2.2	Types of ligand coordination in nanoparticles	10
2.3	Factors influencing the size and shape of nanoparticles	12
2.4	LaMer plot with separated growth stages	13
2.5	Evolution of CdSe absorption and morphology with the additive DCE	16
2.6	Correlation of nanopyramid size and DCE/Cd ratio	18
2.7	Micrographs of CdSe nanopyramids with oleic instead of phosphonic acid	20
2.8	Temporal evolution of absorption maxima with different chloroalkanes	22
2.9	TEM micrographs of samples prepared with DCE, DBE and DIE	23
2.10	Addition of 1-chlorooctadecane after the nucleation	25
2.11	XPS spectra of nanorods and -pyramids	26
2.12	Temporal changes of the elemental composition determined by TXRF	29
2.13	Rod and hexagonal pyramidal geometry with distinct facets	31
2.14	DFT simulations: PPA on different crystal facets	33
2.15	LaMer-type plot of the CdSe nanopyramid formation reaction	34
2.16	Plot of the pH of aliquots versus time	36
3.1	Band position and work functions of CdSe and different metals	41
3.2	Modes of epitaxial heterodeposition.	45
3.3	Mechanisms of oligomer formation	46
3.4	Scheme of reactive sites of CdSe nanopyramids.	51
3.5	Micrographs of nanopyramids with cluster sized Au domains	52
3.6	Au domain growth and absorption spectra with increasing Au/CdSe ratio	55
3.7	Photographs of Au precursor solutions	57
3.8	HR-TEM micrographs of CdSe nanopyramids with Au shell and dots.	59
3.9	IR-spectra of CdSe nanopyramids before and after treatment with dodecanethiol	60

3.10	X-ray diffraction pattern of Au-CdSe shell nanoparticles	62
3.11	Atomic ratios and diameters of Au-CdSe dot and shell samples	63
3.12	XPS survey spectra of CdSe and Au-CdSe nanoparticles	65
3.13	XPS data of Se 3d and Au 4f regions of Au-CdSe samples with shell and dots.	67
3.14	TEM micrographs of annealed Au-CdSe films	70
3.15	TEM micrograph of nanopyramids after ion exchange with Ag.	72
3.16	Diffraction pattern after ion exchange from Cd to Ag	73
3.17	TEM micrographs of CdSe nanopyramids at different stages of cation exchange with Pd	74
3.18	High resolution micrographs, EDX mapping and electron diffraction of CdSe- Pd _x Se _y nanoparticles	76
3.19	Evolution of absorbance spectra during an ion exchange reaction between Cd and Pd	78
3.20	Oligomeric Pt-CdSe nanoparticles with different Pt domain sizes	79
3.21	Absorbance and emission of Pt-CdSe samples	80
3.22	Electron diffraction and interface regions of Pt-CdSe nanoparticles	81
3.23	EDX map of Pt-CdSe hybrid nanoparticles.	81
3.24	TEM micrographs of <i>in situ</i> annealed Pt-CdSe nanoparticles	83
3.25	High resolution micrographs of annealed Pt-CdSe nanoparticles	84
4.1	Scheme of a nanoparticle based source-drain device	88
4.2	Coulomb blockade	90
4.3	Electron transport mechanisms in disordered semiconductors	91
4.4	Band structures and charge transport at metal-semiconductor junctions	95
4.5	Interdigitated array electrodes	97
4.6	Micrographs of a CdSe nanopyramid array	99
4.7	Current-voltage curves of a CdSe nanopyramid device	100
4.8	Micrographs of Pt-CdSe nanoparticles and devices	102
4.9	Dark and photocurrent of Pt-CdSe arrays (Pt= 1.7 nm)	103
4.10	Dark and photocurrent of Pt-CdSe arrays (Pt= 3.2 nm)	105
4.11	Fits of current-voltage curves of Pt-CdSe arrays	106
4.12	Temperature dependence of dark currents (Pt= 3.2 nm)	109
4.13	Possible paths for electron transfer in Pt-CdSe arrays	110
5.1	Lengths in hexagonal (di)pyramids	127

A.1	Temporal evolution of absorbance and emission in a reaction with DCE . . .	I
A.2	Morphological evolution without additive	I
A.3	Optical and morphological evolution in reactions with chloroalkanes	II
A.4	Electron beam induced migration in Au-CdSe samples	III
A.5	XPS Se 3d signal of a Au-CdSe shell sample	III
A.6	Beam current dependency of migration in Au-CdSe samples	IV
A.7	Composition of nanoparticles after ion exchange with Ag	IV
A.8	Evolution of absorbance spectra of CdSe nanopramids incubated with Pd at room temperature	V
A.9	X-ray diffraction pattern of Pt-CdSe nanoparticles	V
A.10	Electrode with CdSe nanopyramid array after annealing.	VI
A.11	Schematic depiction of a 4-point probe measurement	VI
B.1	GHS-pictograms	XXI

List of Schemes

3.1	Au deposition onto CdSe nanoparticles in the presence of amine ligands . .	53
-----	--	----

List of Tables

2.1	Nanoparticle dimensions at different DCE/Cd ratios.	18
2.2	Adsorption energies of ligands on dominant CdSe surfaces	31
3.1	Standard reduction potentials of relevant species	48

3.2	Ionic radii, acid hardness, relevant selenides and their crystal structure(s) of different metal cations	50
3.3	Composition of nanopyrramids before and after reaction with Pd(II)	75
3.4	Atomic composition of CdSe and CdSe-Pt samples determined by EDX. . .	79
4.1	Temperature dependencies of selected electrical transport mechanisms . . .	108
5.1	Details of reactions with different halogenated additives	115
5.2	Details of Au deposition reactions	120
5.3	Parameters for incubation of CdSe nanopyrramids (DCE) with Pd(II) . . .	121
5.4	Parameters for incubation of CdSe nanopyrramids (COD) with Pd(II) . . .	122
5.5	Parameters for incubation of CdSe nanopyrramids (DCE) with Pd(II) 2 . .	122
B.1	Safety information for employed substances	VII
B.2	All H, EUH and P statements	XI

1 Introduction

Based on their outstanding properties, nanoparticles have entered broad areas of research related to (photo)catalysis [1], energy conversion [2], optoelectronics [3], and biomedicine [4, 5]. A major factor determining these properties and the reactivity of nanoparticles is their size and related to it their large surface-to-volume ratio. The small dimensions cause quantum mechanical confinement of electrons and thus altered physical conditions compared to bulk materials [6]. The reduction in size is also advantageous to save precious materials such as catalytic metals. With proceeding climate change and pollution, high hopes rest on developments in solar energy conversion. Nanoparticles offer a variety of solutions for related applications in photovoltaics and photocatalytic conversion of solar into chemical energy.

During the past decades, the preparation of nanostructures consisting of single and multiple components has developed into a tool box for the creation of purpose-designed materials. Especially the colloidal synthesis can be applied to prepare nanoparticles in a large variety of shapes and sizes with comparatively low effort and costs. With the introduction of high temperature preparation methods twenty years ago [7], a way to obtain highly monodisperse nanoparticles was paved. From then on, the control over size and shape of the particles has grown steadily.

Another strong impulse was the selective formation of multicomponent nanostructures that combine materials with different physical properties [8]. In secondary steps other materials can be grown onto prepared nanoparticles with high precision [9, 10]. Metallic nanostructures deposited onto semiconductors, for instance, facilitate the separation of charges that are photogenerated in the semiconductor [11]. This fundamental process is the basis for improved efficiencies in fields such as photocatalytic water splitting [12]. An interesting feature of metal domains on semiconductor nanoparticles is their ability to improve electrical contacts to the latter [13]. This might be utilised to increase the charge transport in semiconductor nanoparticle arrays and affect the photocurrent obtained under illumination.

Creating and characterising such a nanoparticle array requires a high degree of control over all steps involved, from semiconductor synthesis over metal deposition to the final assembly. To reach this control, an understanding of the fundamental processes accompanying each step is necessary. By modulating the shape of the semiconductor material, for example, the number of sites reactive towards the deposition of metals can be varied which affects the whole architecture. Their comparatively large surface results in lowered melting points of nanoparticles and furthermore makes them susceptible for fast dissolution, the adsorption of molecules and reactions with the surrounding medium [14]. To prevent them from coagulation, nanoparticles are coated by a layer of surfactants, also referred to as ligands or stabilisers. Apart from exhibiting a stabilising effect, the adsorption of such ligands may play an important role in the shape evolution of wet-chemically prepared nanostructures. In connection with the preparation of CdSe-carbon nanotube composites 1,2-dichloroethane was observed to induce the formation of hexagonal pyramidally shaped CdSe nanoparticles [15, 16]. A mechanism involving chloride ions was presumed.

The peculiar pyramidal geometry provides a high number of sites prone to metal deposition and is thus an ideal candidate for an envisaged synthesis of hybrid nanoparticles with several defined metal domains in an oligomeric structure. The control of the shape evolution in reactions without carbon nanotubes and a possible adaptation of the method to develop different morphologies is desired. For this reason, a better understanding of the influence of the di-halogen alkane on the shape evolution shall be gained in this work. Another goal is the preparation of hybrid nanoparticles with oligomeric structure for the electrical characterisation in two-dimensional arrays. Finally, the obtained material shall be assembled and pioneering electrical studies shall be conducted to find out how the interplay of the domains influences two-dimensional conductance and the generation of photocurrents.

Following these steps, this thesis is separated into three chapters, each with a theoretical introduction, a results and discussion as well as a conclusions section. In the concluding sections, specific aspects concerning the results of the corresponding chapter will be treated.

In chapter 2, the interactions between ligands and the nanoparticle surface play an important role. The shape control of the semiconductor component by halogenated additives is examined. To better understand why 1,2-dichloroethane induces such a peculiar shape and if the effect may be exploited to tune the size and shape of nanoparticles, experimental and theoretical studies are combined. Systematic variations of halogenated additives as well as elemental and surface analysis are applied. In the theoretical part, calculations

based on the density functional theory and parallels to a classical crystal growth model are presented.

In chapter 3, the seeded-growth deposition of four metals, Au, Ag, Pd and Pt, onto hexagonal pyramidal CdSe nanoparticles in organic solution is examined. The reasons for the formation of a presumed shell-like Au structure with undefined composition observed in preliminary work ([17]) are scrutinised. Among the conducted experiments are studies concerning the influence of the oxidation state of the precursor on the morphology of forming hybrids. The oxidation state of the metal in the shell is examined by X-ray photoelectron spectroscopy. The deposition behaviour of the other three metals is tested by a new common synthetic method with oleylamine as ligand and reducing agent for the metal.

Chapter 4 deals with electrical properties of nanoparticles and specifically two-dimensional Pt-CdSe hybrid nanoparticle arrays. Nanoparticles with two sizes of Pt domains are examined. The assemblies are prepared with the Langmuir-Blodgett technique and measured in a probe station under vacuum. Current-voltage curves are recorded in darkness and under illumination conditions with different irradiation sources. Additionally, the temperature is varied down to cryogenic conditions. In comparison to literature data of related systems observations concerning the transport mechanisms are made.

Experimental details of all chapters are summarised in a joined experimental chapter (chapter 5). A general summary with outlook for the work follows in chapter 6, while chapter 7 contains a summary in German. Additional data for chapters 2, 3 and 4 is provided in the appendix.

2 Halogen induced shape control of CdSe nanoparticles

Due to their special size dependent optical and electronic properties semiconductor nanoparticles find application in photovoltaics [18, 19], (photo)catalysis [1, 12], light emitting devices [20] and biological labelling [21, 22], among others [23].

In these contexts, the shape of the nanoparticles may become important due to physical properties depending on the dimensionality of quantum confinement in the nanostructure or simply their packing behaviour [3, 24, 25, 26]. Apart from their morphology, an aspect that is critical for applications is the passivation of the nanoparticle surface by stabilisers.

Owing to the successful implementation of nanoparticles partially capped by or post synthetically treated with halides into solar cells with increased efficiency [27, 28], incorporation of atomic halogen ligands has attracted much attention recently [29, 30, 31, 32, 33]. In addition to enhancing physical properties in nanoparticle arrays, halides show interesting effects on the shaping of nanoparticles. With metal nanoparticles they are deliberately employed to control the growth with influences on the shape formation [34, 35]. For semiconductor nanoparticles, several cases of wurtzite structures with hexagonal bullet, pyramid, pencil or diamond shape were reported which had in common that chloride precursors were present [36, 37, 38]. A few studies showed an increase of morphological uniformity in branched cadmium chalcogenides with wurtzite arms growing on seeds of deviating crystal structures when halides were added [39, 38, 40]. Juárez and co-workers observed how traces of 1,2-dichloroethane employed as solvent for carbon nanotubes added *in situ* to a synthesis of CdSe nanorods induced a shape evolution [15, 16]. Hexagonal pyramidal nanoparticles with wurtzite structure evolved, which then formed composites with the nanotubes. Chloroalkanes were furthermore reported to aid the preparation of sheet-like lead sulfide nanostructures with the chemical structure of the molecules influencing the dimensions of the crystals [41, 42]. These circumstances built a promising foundation for further studies on the shape control of semiconductor nanoparticles by halogen compounds

with CdSe as a model system with well-known properties. An extension of feasible morphologies presents an attractive goal with respect to increasing demands on the control of nanoparticle shapes for application in thin film arrays or as seed material with controllable reactive sites for heteronanoparticle formation.

In the following, the most important theoretical aspects of the wet-chemical nanoparticle synthesis and methods of semiconductor nanoparticle shape control will be introduced. They will lay the basis for the discussion of aspects of the shape control of CdSe nanoparticles aided by (organo) halogen compounds examined in this work. For more detailed insights into properties and preparation of nanoparticles, references [23, 43, 44, 45, 46] are suggested. A substantial part of the chapter is based on and reproduced in part with permission from [Meyns, M., Iacono, F., Palencia, C., Geweke, J., Coderch, M. D., Fittschen, U. E. A., Gallego, J. M., Otero, R., Juárez, B. H., Klinke, C. *Chem. Mater.* **2014**, *26*, 1813-1821.] Copyright [2014] American Chemical Society.

2.1 Properties and synthesis of semiconductor nanoparticles

The field of semiconductor nanoparticle synthesis offers a wide and growing variety of synthetic protocols and factors that can be tuned to influence and design the dimensions and shapes of the crystals. Known morphologies range from zero- to two-dimensional in terms of bulk-like dimensions (quantum dots [47], nanotubes and nanowires [48, 49], tetrapods [50], nanosheets [51, 52]). This is appealing in so far as the shape of nanoparticles influences physical and chemical properties through changes in electric fields and crystal facet dependent surface reactivity [14, 53, 54, 55].

2.1.1 Properties of semiconductor (CdSe) nanoparticles

In terms of electrical properties, semiconductors take a middle position between highly conducting metals and insulating materials such as glasses or polymers. The reason for this is that they are able to conduct electricity only when activated by thermal energy or light. This additional energy allows electrons to move from the lower valence to the upper conduction band across the band gap; in metals there is no gap between the bands, whereas insulators are defined as having a band gap bigger than 4eV. These bands, formed by energetically close lying electron orbitals, are delocalised over the whole crystal and

excited electron-hole pairs (excitons) are free to move in all directions in bulk materials. In nanoparticles, the number of atoms, each contributing one orbital to the band, is much smaller (between 100 and a few 10000), which causes an increase of the gap with decreasing nanoparticle size and the formation of discrete states at the band edges [6, 24]. At sizes of a few nanometres, the wave functions of electron and hole become confined in the dimensions of the semiconductor nanoparticles, now called quantum dots, and the gap is strongly size dependent (quantum size effect). The number of nanoparticle dimensions ranging in the confinement regime determines the density of available energetic states. This way, the shape and directed growth of a nanostructure may influence its band gap [56]. In spherical nanoparticles all three dimensions are affected and the electronic levels develop into discrete states. This is visible by blue shifts in absorption and emission spectra, in which the first maximum at lower wavelengths in the absorption spectra can be employed to directly relate size and band gap of the nanoparticles [57, 58]. Due to the high surface-to-volume ratio, the configuration of the outer layer of atoms and the ligand sphere protecting the nanoparticles from coagulation make a large impact on the overall properties. For example, the quantum yield of emission and the electrical transport in nanoparticle arrays can be significantly deteriorated by charge trapping sites in form of dangling bonds.

The medium valued direct band gap of II-VI semiconductor CdSe (1.74 eV in bulk [59]) makes it one of the few materials whose nanoparticles can be tuned in size to absorb and emit light throughout the visible spectrum. The electrical properties of CdSe nanoparticles will be addressed in Chapter 4. CdSe crystals occur in the cubic zinc blende or in the hexagonal wurtzite structure. The latter is depicted in Figure 2.1. At room temperature the cubic phase is slightly more stable by 1.4 meV per atom [61]. Polytypism occurs at higher temperatures and the crystal structure depends on the reaction conditions. In the presence of halogens a preferential formation of the wurtzite phase was observed, the reason for which has not been clarified so far [40, 62, 63]. The wurtzite structure is anisotropic, which becomes apparent by differences in the number of bonds per element when counting in opposite directions of the c -axis. In the positive direction Cd has one bond pointing upwards whereas Se has three. For this reason, hexagonal CdSe crystals are usually terminated by a positively charged Cd-rich (0001) and a negatively charged Se-rich (000 $\bar{1}$) facet to minimise the number of dangling bonds [64, 65, 66]. This anisotropic charge distribution creates a dipole moment in the nanoparticles [67, 68].

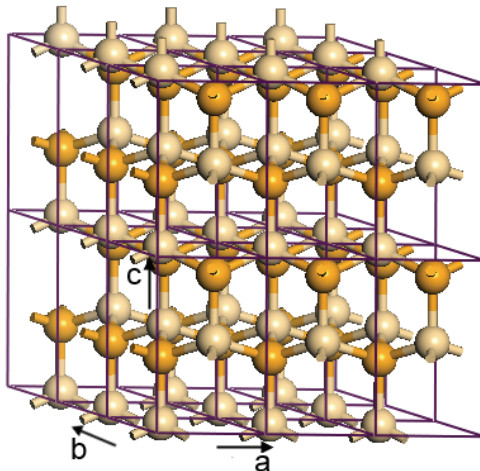


Figure 2.1: Hexagonal wurtzite crystal structure of CdSe composed from unit cells with the lattice constants a , b : 4.30 Å, c : 7.01 Å [60]; Cd atoms are beige, Se atoms are orange. The upper (0001) layer consists of Cd-atoms with one dangling bond, the lower (000 $\bar{1}$) facet is usually terminated by Se with one dangling bond. Created with *Materials studio*.

CdSe nanoparticles alone or as cores coated with inorganic or organic shell materials, are applied in solar cells [18], light emitting diodes [20], and biological imaging [4]. Furthermore, they have acted as model systems for the exploration of properties in a variety of contexts. Among these are optical and electrical studies as well as investigations of shape control during synthesis [69, 70, 71].

2.1.2 Colloidal semiconductor nanoparticle synthesis and shape control

For further processing and efficient applications nanoparticles should be homogeneous in their size and shape. The method of choice to obtain nanoparticles with the highest precision in terms of size and shape is the wet-chemical bottom-up approach, where crystals are prepared from molecular precursors of the components. Semiconductor nanoparticles with small size distributions of below 10% are mainly obtained by hot-injection syntheses with separated nucleation and growth stages as pioneered by Murray, Norris and Bawendi in 1993 [7]. Before going into detail, the basics of nanoparticle formation and different models of shape control will be presented briefly.

2.1.2.1 Basics of nanoparticle nucleation

For the formation of nanoparticles starting materials are mixed and react to a solute form of the crystal¹, not yet considered as a solid phase, which evolves into nuclei once a critical supersaturation is reached. The activation energy necessary for nucleation is provided when the change of the overall free energy

$$\Delta G = -\frac{4}{V_{m,NP}}\pi r^3 k_B T \ln(S) + 4\pi r^2 \gamma \quad (2.1)$$

reaches a maximum. In Equation (2.1) $V_{m,NP}$ is the molecular volume of the material in the crystal, r is the radius of the spherical nuclei, k_B is the Boltzmann constant, S is the saturation ratio and γ is the surface free energy per unit surface area [14]. The maximum is reached for a critical radius r^* when the saturation ratio $S = \frac{c_{solute}}{k_{sp}}$ with the solute concentration c_{solute} and the solubility product of the crystal material k_{sp} is larger than one [72]. The critical radius is obtained as

$$r^* = \frac{2V_{m,NP}\gamma}{3k_B T \ln(S)} \quad (2.2)$$

by derivation of Equation 2.1. During nucleation, the supersaturation depletes until no further nuclei form. These nuclei continue to grow towards nanoparticles whose size and shape can be controlled by growth parameters such as concentration, temperature and the choice of ligands. Finally, the solute concentration will approach the level of the material's solubility and the critical radius will shift to larger values so that smaller particles dissolve in favour of further growth of bigger ones, a process known as Ostwald ripening [73].

2.1.2.2 Mechanisms of shape control

Non-spherical shapes form whenever the facets of a crystal exhibit different growth rates; fast growing facets are eliminated and slowly growing facets eventually determine the shape or *Tracht*, the entirety of the facets that form the crystal surface. Growth rates can be governed by thermodynamic or kinetic influences, depending on the growth conditions. Apart from temperature and concentration, a major role in size and shape control is played by

¹ In literature the terms *solute* and *monomer* are employed to describe a small unit consisting of at least one of each crystal components. Solute is the term found in works on classical crystal growth and is less limited, since the solute form must not necessarily be a single formula unit.

organic surfactants, which are employed to stabilize the solid nanoparticle phase against dissolution and coagulation [74, 75, 76]. The most commonly employed types of ligands to stabilise semiconductor nanoparticles are amphiphilic organic molecules counted to the groups of neutral L-type or negatively charged X-type ligands. The first group may coordinate both cationic and anionic crystal components, while the second one selectively balances positively charged surface atoms to reach overall charge neutrality. If both types are present, the interaction with X-type ligands will dominate due to stronger interactions with the surface [29, 31, 77, 78]. L-type ligands provide additional stability but are more easily washed away during purification. A breakthrough observation regarding selective X-type adsorption is the case of phosphonic acid impurities in a CdSe synthesis with otherwise neutral tri-*n*-octylphosphane (TOP) ligands in tri-*n*-octylphosphane oxide (TOPO), which coordinated the nanoparticles in form of phosphonates [79]. As mentioned earlier, halide ions acting as atomic X-type ligands gain increasing popularity.

The terms *surfactant*, *stabiliser* and *ligand* are often used interchangeably in the literature. Since surfactants and stabilising molecules usually are amphiphilic compounds with alkyl chains, the term ligand will be applied here within the meaning of a potentially surface bound constituent including short molecules and halides.

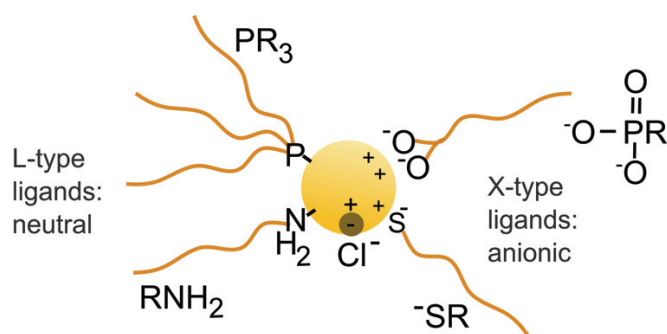


Figure 2.2: Most of the ligands employed in semiconductor nanoparticle stabilisation belong to the groups of neutral L-type ligands, which bind to cations and anions of the crystal (a dative bond to the metal cation is shown here), and X-type ligands that selectively bind to the cationic component. The named examples are tri-*n*-alkylphosphanes (R_3P), primary amines (RNH_2), thiolates (RS^-) and phosphonates ($(RPO_3)^{2-}$). Halides can act as atomic X-type ligands. In metallic nanoparticles with negative surface charges cationic ligands are another important group of surfactants.